Extracting seismic uncertainties from tomographic velocity inversion and their use in reservoir risk analysis

Jérémie Messud[1], Mathieu Reinier[1], Hervé Prigent[1], Patrice Guillaume[1], Thierry Coléou[1], and Sylvain Masclet[1]

Abstract

Structural information in subsurface seismic images is critical for reservoir delineation, reserve estimation, and well planning. However, by its very nature, it is also uncertain. One cause of the image uncertainty is the migration velocity model that directly affects the position of migrated events, both laterally and vertically. (The term "velocity" is meant in the broad sense; i.e., it also includes the anisotropy parameters.) We present a method that accounts for uncertainties in a velocity model estimated by tomography and translates them into the migrated domain. Standard-deviation attributes on target horizon positions or layer thicknesses are extracted. The method includes quality controls for validating the estimated uncertainty attributes before integration with other downstream or interpretative information. The method is demonstrated on a North Sea area covered by data from multiple seismic surveys. We observe that uncertainties increase with model complexity or depth and decrease as the illumination diversity increases. The computed uncertainty maps constitute a valuable source of information for hierarchizing (both qualitatively and quantitatively) different areas in the survey. For the purpose of reservoir risk analysis, we combine our technique with other information (e.g., interpretation uncertainties) to map how uncertainties in the depth of the structural spill point impact the gross rock volume (GRV) estimation of a reservoir.

Introduction

All processes used to infer information about a real-world system containing noise are subject to uncertainties. This is no different in the field of seismic where information in acquired seismic data often is used to drive a model-based inversion. An example of such a process (and the one we will discuss in this paper) is velocity-model estimation via tomography. (Note that the term "velocity" is meant in the broad sense; i.e., it also includes the anisotropy parameters.) Here, it is well known that the input data, modeling, and a priori or regularization inversion elements are not an entirely accurate description of the real earth. For instance, residual moveout information, namely the deviation of an event in a common-image gather from the ideal flat situation, carries an uncertainty related to both the size of the wavelet of the picked event and the intrinsic data quality that varies by location in the data. Thus, the subsurface model estimated by tomography (or other inversion methods) is not the true subsurface velocity, or even the optimum migration model, but is instead a representation of our knowledge about them. In fact, Tarantola (2005) describes the model obtained from a tomographic process as the "maximum-likelihood" (or most probable) model with respect to the supplied inversion data, assumed physical model, and a priori information. Hence, tomography-model uncertainties can be considered as "error bars" around this "maximum-likelihood" model. If all underlying assumptions are met, then clearly such error bars represent vital information in two respects: (1) the reliability of the inversion result itself and (2) what the true or optimum model could be because it is expected to be within these error bars.

A migration with the maximum-likelihood tomographic velocity model can be considered as giving the maximum-likelihood migrated image, with uncertainties in this velocity model contributing to uncertainties in the migrated domain. Such uncertainties directly affect lateral and vertical migrated event positions. Important information for reservoir exploration and development is the uncertainty in the structural aspect of the seismic image, in particular the key target horizon (reflector) positions. The information derived from our tomography-based uncertainty analysis helps quantify horizon and fault-position errors, as well as layer-thickness errors. This information can serve several purposes in risk evaluation of a potential hydrocarbon prospect:

- It improves our understanding and confidence in the final depth-migrated image, discriminating between more accurately imaged areas and areas with reduced confidence in the image.
- Once translated into depth standard-deviation maps, the uncertainties can be integrated with other information for risk assessment of, for example, depth prediction, reservoir delineation, reserve estimation, GRV evaluation, and well-placement optimization.

In the first part of this paper, we present our method for estimating uncertainties in the tomography velocity model. The method provides qualitative and quantitative information associated with the positioning errors in seismic depth-migrated images. The method is then applied to data from a North Sea area covered by multiple seismic surveys, and we subsequently interpret the results. Finally, using this data set we discuss an application of the estimated depth uncertainties to highlight the influence of the structural spill point on a reservoir's GRV estimation.

Method for estimating uncertainties in a tomography model

We start this section with some clarifications of our use of the term "uncertainties":

- We assume the maximum-likelihood model has been obtained by a nonlinear slope tomography with tilted transverse isotropy (TTI) (Montel et al., 2010; Guillaume et al., 2013). Uncertainties relating to velocity-model parameters can be evaluated by developing a probability density function (PDF) around this maximum-likelihood model.
- The PDF is assumed to have a Gaussian distribution in a sufficiently large interval around the maximum-likelihood position (Tarantola, 2005).
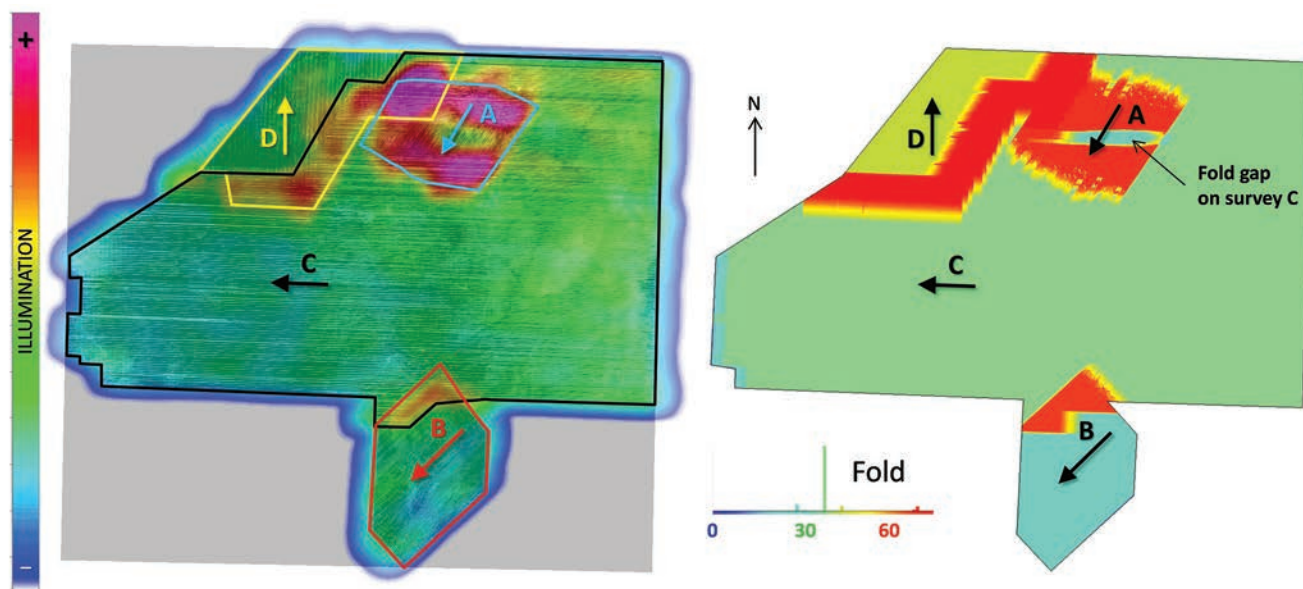
Figure 1. Combined coverage of the four different surveys (A–D): (left) illumination map, where the hot and cold colors indicate high and low illumination, respectively, and (right) acquisition bin fold, with a maximum fold of ~75. Note that the shooting direction of each survey is indicated by the direction of the associated arrow.

- We consider a 68.27% confidence interval that represents a standard-deviation confidence interval for a Gaussian PDF.
- Uncertainties in the spatial position of migrated reflectors are assumed to be due largely to uncertainties in the tomography velocity model used by the imaging algorithm. Migration data uncertainties relating to, for example, noise, multiples, or variable illumination are not taken into account for now.

For the final goal of reservoir risk analysis, we wish to compute standard-deviation-like quantities on horizon positions (x, y, depth). Our method involves three steps:

1) Generate a series of tomographically consistent model perturbations that are within a standard-deviation confidence interval. Our tomography model space is described by cardinal cubic B-splines (with a range of 500,000 to 50 million parameters). We use nonlinear slope tomography (Guillaume et al., 2013) where the linear system to be solved is made up of both a data misfit term and all additional constraints. From this system, we can generate equiprobable velocity-model perturbations by exploring the envelope of the standard-deviation confidence interval. The envelope represents a "hyper-ellipsoid contour" of the PDF (Duffet and Sinoquet, 2006). This step involves the tomography a posteriori covariance matrix (Pratt and Chapman, 1992; Zhang and McMechan, 1995; Tarantola, 2005) and a random sampling of the contour. The a posteriori covariance matrix (defining the uncertainty range) contains, in particular, information relating to data quality and tomography constraints.

With respect to the assumed model and the tomography process, the method accounts for the model subspaces "resolved" and "unresolved by the tomography." The "unresolved" subspace is defined by the basis vectors corresponding to the smallest eigenvalues (Pratt and Chapman, 1992). We can separate the uncertainties relating to the subspace resolved by the tomography from the total uncertainties spanning the full model space (namely the union of the resolved and unresolved subspaces). The total uncertainties highlight, among other things, the quality of the illumination. Uncertainties relating to the subspace resolved by the tomography are a subset of the total uncertainties that give complementary information in better-illuminated areas. This concept will be illustrated using a North Sea data example.

Other strategies for exploring the model space are already used in the seismic industry. For example, Osypov et al. (2013) propose a method to sample the PDF of the solution of a tomographic problem constrained by steering filters.

2) Migrate target horizons in the computed perturbed models. The key target horizons are kinematically migrated at zero offset for every equiprobable perturbed velocity model computed from the tomography-derived equations (Duffet and Sinoquet, 2006). For each horizon, this leads to a set of possible (x, y, depth) locations of this horizon that are used in subsequent analyses.

3) Compute "standard deviations" on horizon position. The maximum possible variation in each horizon position is related to the standard-deviation confidence interval on the depth-migrated positions. Hence, we can compute standard-deviation-like *depth* attributes that account for the information in a posteriori covariance matrix of the tomographic inverse problem and of the kinematic migration problem (in the linearized approximation). The same method can be applied to the x and y components of the horizon positions: lateral displacements are computed by breaking down the horizon into locally coherent reflecting events (characterized by their position and dip) and by tracking their individual lateral displacements from one kinematic migration to the other.

North Sea real data example

The method described above is now illustrated on a North Sea real data example. Four different surveys (labeled A–D in

Figure 1) were acquired over the years by different contractors. Each survey was shot with a different main acquisition direction or azimuth (illustrated by the arrows in Figure 1a) and its own specific recording configuration ranging from one to six cables. A specific processing challenge for such a multisurvey project is to provide a seamless merged volume in terms of amplitude, phase, and positioning. Fortunately, in our case, the matching process was eased by significant overlaps of double-azimuth coverage between the surveys. A triple overlap is also noticeable between surveys A, C, and D (Figure 1a). Note that survey C is more recent than survey A and features a "no data" zone around a rig location (highlighted in Figure 1b).

Figure 2. The maximum-likelihood prestack depth migration velocity model overlain with a subset of 20 (among several hundred) random migrated horizons from the perturbed models.

A geologically plausible prestack depth migration model was built using multilayer nonlinear slope tomography (Guillaume et al., 2013), and the resulting maximum-likelihood model showed excellent well ties at wells distributed homogeneously throughout the survey area. To initiate the tomography-derived uncertainty analysis, 500 tomographically consistent and equiprobable perturbations were generated around the maximum-likelihood velocity model within a standard-deviation confidence interval. All key horizons (namely the layer boundaries in our multilayer tomography context) were repositioned in the perturbed models by zero-offset kinematic migrations. A representative subset of horizon realizations is displayed on the velocity model allowing a first glimpse at our "confidence interval" (Figure 2). It shows how the morphology of the main horizons can vary and how some localized features can appear, move, or even disappear from one realization to another while honoring the inversion data input to the slope tomography.

Statistical attributes can be mapped onto the horizons to allow easier quality control of the global results. Figure 3 shows an example of these attributes at the top chalk level where, in general, we observe that the depth range of different realizations tends to increase with depth and structural complexity in the overburden. A clear correlation can be observed between the illumination map in Figure 3a and the total uncertainty map in Figure 3c. Specifically, areas with overlapping surveys that provide multiazimuth illumination show lower uncertainties. In addition, lower-fold areas such as the rig zone affecting survey C cause relatively higher uncertainties correlated to the reduction in tomographic rays (and angular diversity) in this area. Also, as would be expected, we observe larger total uncertainties on the survey edges.

Figure 3d shows the contribution of uncertainties associated with the subspace resolved by the tomography. This attribute, among others, highlights how illumination diversity drives the discrimination power of the tomographic process, with a reduced uncertainty clearly visible along the corridor of overlap between surveys C and D, these two surveys having perpendicular acquisition directions. We also mention that a correlation can be observed between the large values in the eastern part of survey C and the increased depth of the top chalk horizon in Figure 3b.
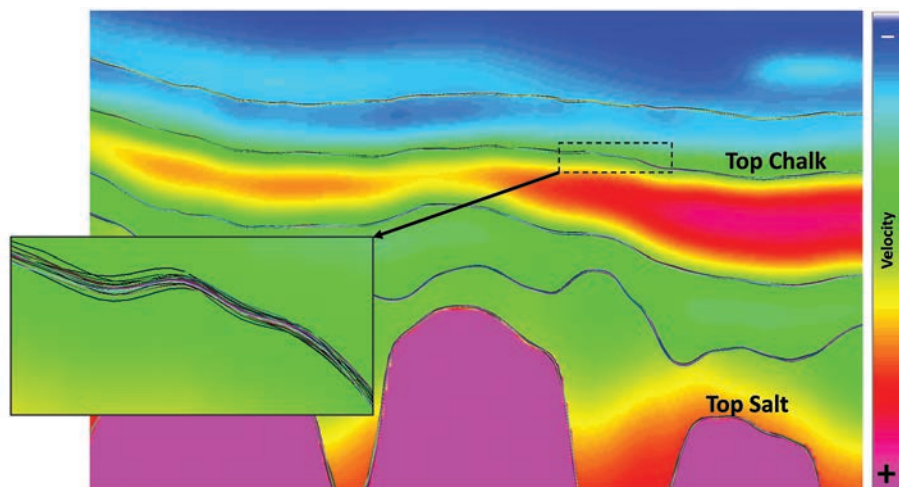
For further insight into these results we note that, on one hand, the total uncertainty highlights the acquisition illumination and structural complexity. On the other hand, the subspace resolved by the tomography exhibits interesting low-amplitude, spatial variations of the uncertainty. In well-illuminated areas, those uncertainties will also vary with the reliability and richness of the picked residual moveout information that feeds the tomography. Interestingly, survey B features shorter cables, and the lack of long-offset recording coincides with a clear increase in uncertainty in the southern edge of the area (Figure 3d). Similarly, the most recent survey D with a higher number of cables (six) resulted in less populated short offsets at outer cables: as a result, we observe an increased uncertainty in the northwest corner (Figure 3d) when compared to the average uncertainty on, for example, survey C, which had only three cables.

Figure 4 shows 3D displays of the top and base salt horizons overlain with the total depth standard deviation. From this, we see larger total uncertainties in poorly illuminated areas such as the steeply dipping structural flanks and observe that the uncertainties computed for these dipping events also depend on the shooting direction relative to these structures. Again, specifically, the steep salt flanks in Figure 4a and the faults in Figure 4b consequently have significantly larger uncertainty values. This is even more critical when the shooting direction is not perpendicular to the strongest dips (Figure 4b): Maximum raypath diversity is obtained in the acquisition direction (which usually corresponds to the direction of maximum complexity in the subsurface), thus reducing velocity uncertainties in that direction.

Risk analysis from uncertainty information on GRV estimation

Uncertainties are not absolute values but need to be translated into something useful for a given target. The information derived from the tomography uncertainty analysis must fit into a larger uncertainty evaluation targeting a particular problem (Coléou, 2001). Attribute maps of the standard deviation for selected horizons can be computed for the depth and, also, for other
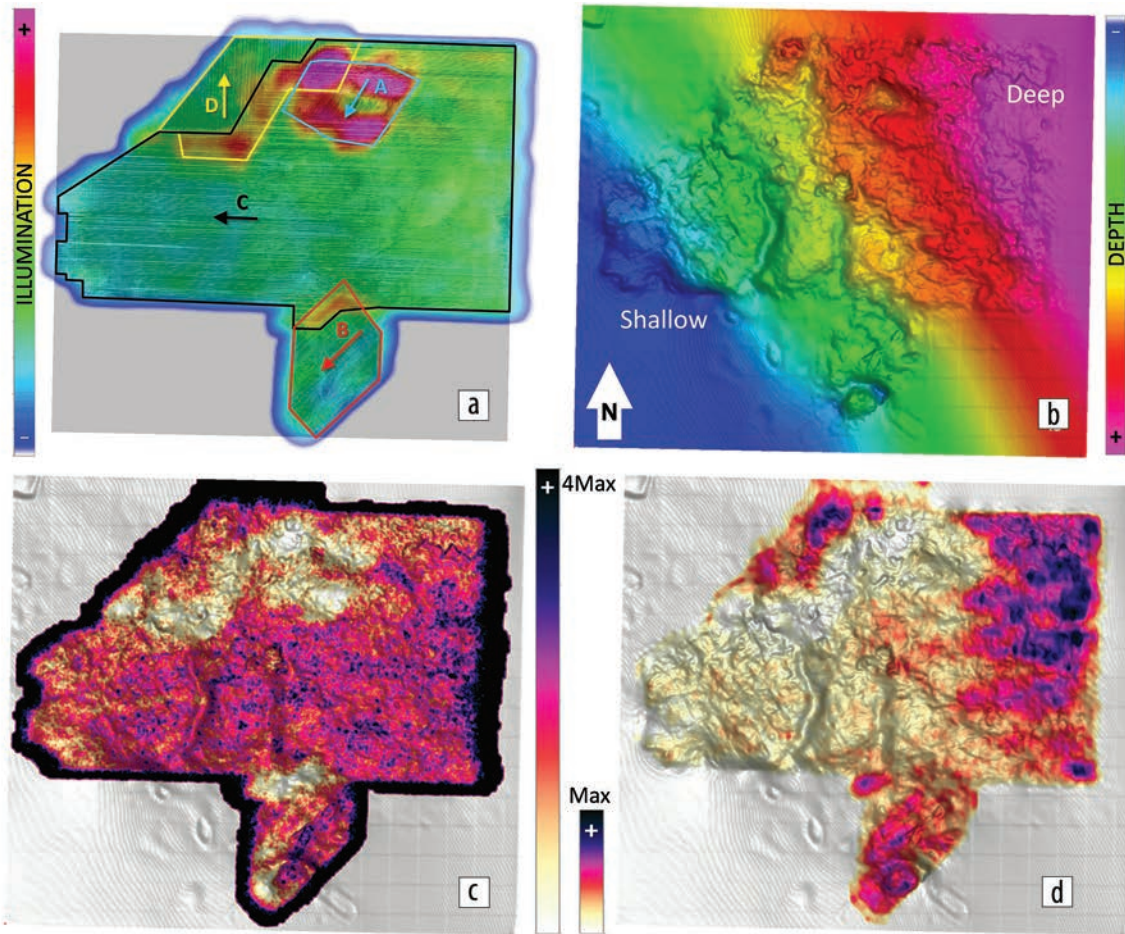
Figure 3. Top chalk horizon attributes: (a) illumination map, (b) horizon depth, (c) total depth uncertainties (the *z*-direction standard deviation), and (d) standard deviation from the contribution of the subspace resolved by the tomography. Note that panels 3c and 3d use the same color map but with different scale ranges.
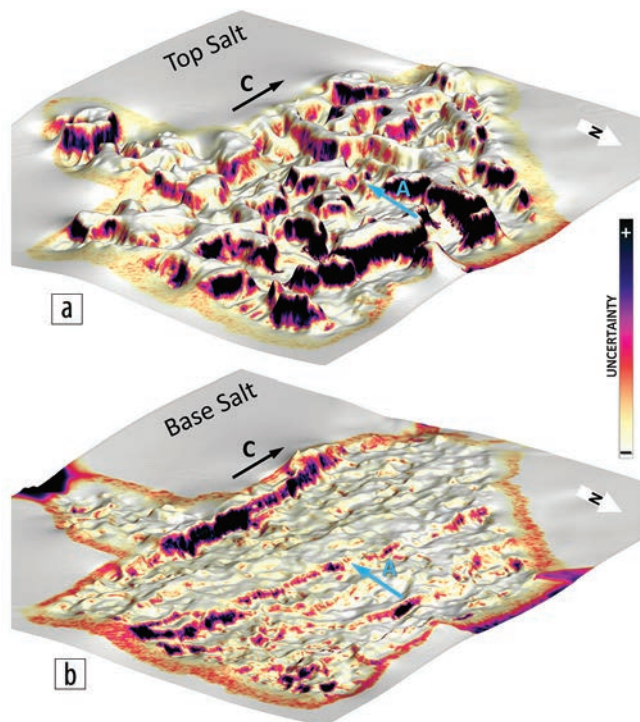
Figure 4. 3D displays of (a) top salt and (b) base salt overlaid with the total depth uncertainty (the *z*-direction standard deviation). Note the increased *z*-direction standard deviation along the steep dipping structural flanks and faults where small lateral positioning errors result in large depth uncertainties.
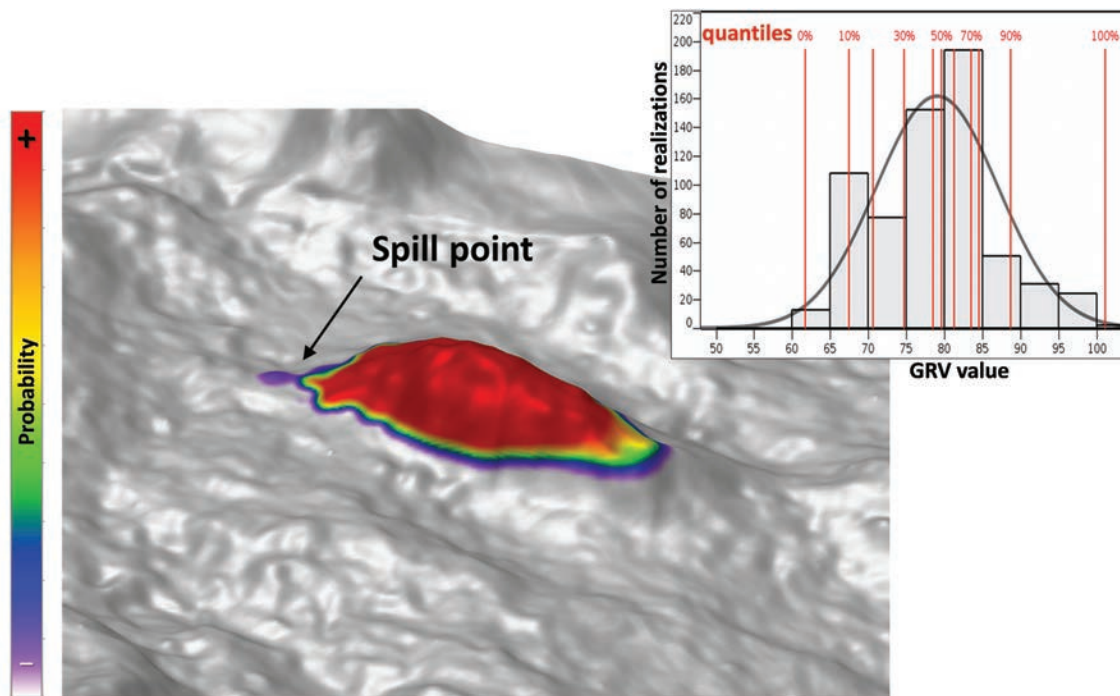
Figure 5. Probability of prospect outline being above the spill point (colored; red is a probability of one) and GRV histogram. The horizontal axis of the histogram defines the GRV value classes (units are not shown), and the vertical axis defines the number of realizations per class; realization quantiles are indicated by the red bars.

attributes such as lateral x, y positioning or thickness. Computed standard-deviation maps are all the more relevant as they can be directly integrated in the risk assessment of, for example, depth prediction, GRV evaluation, pore-pressure prediction, and well-placement optimization, to help reduce the exploration risks.

One element in the uncertainty of the structural closure of an exploration prospect is the uncertainty in the interpretation. However, this is also influenced by the uncertainty in the image, which obviously relates to the uncertainty in the tomography model that generated this image, impacting the spill point depth and position, and therefore the GRV estimation. For a specific area of interest in our North Sea example, Figure 5 shows the probability map to be above the spill point and the corresponding GRV histogram. Uncertainties in the tomographic velocities are used to generate the different realizations along with other sources of uncertainties to obtain these results.

In this example, we combined the z-direction standard deviation for the top reservoir surface (evaluated from the velocity uncertainties) with the interpretation uncertainties to generate a number of possible realizations of the top reservoir surface. The prospect, a four-way dip-closure, is bound by a spill point. The spill point is computed for each realization, giving the maximum depth of the hydrocarbon contact, the outline of the prospect, and the corresponding GRV. This result enables us to produce a map of the probability of the reservoir top to be above the contact (left of Figure 5). The probability attribute is overlaid onto the top reservoir surface of the maximum-likelihood model. The histogram of the GRV values for the realizations for subsequent reserve uncertainty evaluation and economic risk analysis is shown top right of Figure 5. In our example, the uncertainty analysis leads to gross volume values between 62 and 102, with P10 (minimum case) at 67, P90 (maximum case) at 89, and P50 (base case) at 78.

In this exploration case, where no well has yet been drilled on the prospect, the geometry of the prospect is the main ranking criterion for in-situ reserve evaluation as net-to-gross, porosity, saturation, and other information needed have not yet been measured. The velocity uncertainties have a critical place in this process.

It is important to deliver uncertainties in such a way that they can be integrated with other information in a risk-assessment study. The best solution among the various integration possibilities available is to adapt the uncertainty attributes to the specific requirements of the problem to hand. For example, this uncertainty attribute could be the standard deviation of an event's vertical depth, as illustrated in our example, or a layer thickness, but also errors on the lateral position of a sealing fault.

Conclusion and outlook

We have presented a method for: (a) computing uncertainties in tomography velocity models derived from surface seismic data and (b) translating them into the migrated image domain. Standard deviations on horizon depth positions or layer thicknesses are extracted from statistical analysis of the different uncertainty realizations. We have illustrated this technique on a North Sea data example involving a velocity model with tilted transverse isotropy and shown that the computed uncertainties do indeed follow the anticipated behavior caused by expected inaccuracies in the tomographic process. Specifically, these uncertainties increase with model complexity or depth and decrease as the illumination diversity increases. As such, these uncertainties constitute a valuable source of information for qualitative comparison between different areas in the survey. Finally, we have demonstrated quantitative integration of these uncertainties with other information for reservoir risk analysis, in particular, depth prediction and gross rock volume evaluation. Seismic uncertainty analysis is an

expanding area of active research in both academia and industry. There is growing acceptance of the benefits that it can bring in risk estimation during the exploration and development cycle. We believe this work represents a step along this path. **TLE**

Corresponding author: jeremie.messud@CGG.com

References

Coléou, T., 2001, On the use of seismic velocities in model building for depth conversion: 63rd Conference and Exhibition, EAGE, Extended Abstracts, IV–1.

Duffet, C., and D. Sinoquet, 2006, Quantifying uncertainties on the solution model of seismic tomography: Inverse Problems, **22**, no. 2, 525–538, http://dx.doi.org/10.1088/0266-5611/22/2/009.

Guillaume, P., X. Zhang, A. Prescott, G. Lambaré, M. Reinier, J.-P. Montel, and A. Cavalié, 2013, Multi-layer non-linear slope tomography: 75th Conference and Exhibition, EAGE, Extended Abstracts, Th 04 01, http://dx.doi.org/10.3997/2214-4609.20130032.

Montel, J.-P., P. Guillaume, G. Lambaré, and O. Leblanc, 2010, Non-linear slope tomography: extension to MAZ and WAZ: 72nd Conference and Exhibition, EAGE, Extended Abstracts, P257, http://dx.doi.org/10.3997/2214-4609.201401159.

Osypov, K., Y. Yang, A. Fournier, N. Ivanova, R. Bachrach, C. E. Yarman, Y. You, D. Nichols, and M. Woodward, 2013, Model-uncertainty quantification in seismic tomography: method and applications: Geophysical Prospecting, **61**, no. 6, 1114–1134, http://dx.doi.org/10.1111/1365-2478.12058.

Pratt, R. G., and C. H. Chapman, 1992, Traveltime tomography in anisotropic media-II: Application: Geophysical Journal International, **109**, no. 1, 20–37, http://dx.doi.org/10.1111/j.1365-246X.1992.tb00076.x.

Tarantola, A., 2005, Inverse problem theory and methods for model parameters estimation: Society for Industrial and Applied Mathematics, http://dx.doi.org/10.1137/1.9780898717921.

Zhang, J., and G. A. McMechan, 1995, Estimation of resolution and covariance for large matrix inversions: Geophysical Journal International, **121**, no. 2, 409–426, http://dx.doi.org/10.1111/j.1365-246X.1995.tb05722.x.